

# Oxygen Selective Ceramic Hollow Fiber Membranes for Partial Oxidation of Methane

Haihui Wang

The Key Lab of Enhanced Heat Transfer and Energy Conservation of Chinese Ministry of Education, School of Chemistry and Chemical Engineering, South China University of Technology, Guangzhou 510640, China

Armin Feldhoff and Jürgen Caro

Institute of Physical Chemistry and Electrochemistry, Leibniz University of Hannover, Callinstr 3-3A, D-30167, Hannover, Germany

Thomas Schiestel

Fraunhofer Institute of Interfacial Engineering and Biotechnology (IGB), Nobelstr. 12, D-70569, Stuttgart, Germany

Steffen Werth

Uhde GmbH, Friedrich-Uhde-Str, 15, D-44141, Dortmund, Germany

DOI 10.1002/aic.11856

Published online July 13, 2009 in Wiley InterScience (www.interscience.wiley.com).

*A  $\text{BaCo}_x\text{Fe}_y\text{Zr}_{2-x-y}\text{O}_{3-\delta}$  (BCFZ) perovskite hollow fiber membrane was used to construct reactors for the partial oxidation of methane (POM) to syngas. The performance of the BCFZ fibers in the POM was studied (i) without any catalyst, (ii) with catalyst-coated fibers, and (iii) with catalyst packed around the fibers. In addition to the performance in the POM, the stability of the BCFZ hollow fiber membranes was investigated for the different catalyst arrangements. Best stability of the BCFZ hollow fiber membrane reactor in the POM could be obtained if the reforming catalyst is placed behind the oxygen permeation zone. It was found that a direct contact of the catalyst and the fiber must be avoided which could be achieved by coating the fiber with a gold film. © 2009 American Institute of Chemical Engineers AICHE J., 55: 2657–2664, 2009*

*Keywords: perovskite, hollow fiber, mixed conductor, membrane reactor, POM*

## Introduction

Large amounts of natural gas resources are still not utilized due to their remoteness and the small scale of the individual gas fields (so called stranded gas resources). According to estimates, these stranded gas resources account to roughly 60% of the available gas resources<sup>1</sup> and today

these resources are usually flared or reinjected in associated oil fields to increase oil recovery. Gas-to-Liquids (GTL) technologies like Fischer-Tropsch-Synthesis (FT)<sup>2</sup> can convert such stranded gas reserves into easily transportable liquid fuels. FT consists of three stages, the synthesis-gas (a mixture of  $\text{H}_2$  and CO) generation, the production of higher hydrocarbons and waxes in a Fischer-Tropsch-synthesis step, and the upgrading of the heavy products by catalytic hydro cracking. The synthesis-gas generation usually done by autothermal reforming or steam-reforming accounts to a significant part of the total investment and operational costs<sup>3</sup>

Correspondence concerning this article should be addressed to H. Wang at hhwang@scut.edu.cn

so its optimization has a large impact on the applicability of the FT process. The partial oxidation of methane (POM) is a promising alternative for syngas generation because it is a mildly exothermic reaction and could produce syngas with the  $H_2/CO$  ratio of 2:1, which is a preferable feed stock for methanol synthesis or the Fischer-Tropsch reaction. However, due to commercial reasons, nitrogen in the syngas must be avoided, so applicability of POM depends on the availability of cheap oxygen. Recently developed ceramic membrane reactors can integrate oxygen separation and POM into a single step and therefore show a great potential for the cost reduction of syngas generation.<sup>4</sup>

For practical applications, a dense oxygen selective membrane has to show (1) stability for long-term operation at elevated temperatures ( $>800^\circ\text{C}$ ) under strongly reducing atmospheres such as the mixture of carbon monoxide and hydrogen, (2) considerable high oxygen permeability under operation conditions, and (3) the necessary strength to withstand the mechanical stress in the membrane reactor. Furthermore, the material and the membrane should be cheap enough for large-scale industrial applications. To fulfil these requirements, extensive R&D work has been performed since Teraoka et al. published their first article on the oxygen permeability through  $La_{1-x}A_xCo_{1-y}Fe_yO_{3-\delta}$ .<sup>5</sup> For example, Yang's group has developed a novel material named  $Ba_{0.5}Sr_{0.5}Co_{0.8}Fe_{0.2}O_{3-\delta}$ , which shows high oxygen permeability and good operational stability under POM reaction conditions.<sup>6,7</sup> To further improve the stability of the membrane materials, ions with constant valence ( $Zr^{4+}$ ,  $Ga^{3+}$ ,  $Al^{3+}$ )<sup>8-13</sup> were used to partially substitute reducible B-site ions ( $Co^{3+}$ ,  $Fe^{3+}$ ). Recently, several cobalt-free perovskite materials were reported to meet the stability requirements under reducing environments. However, the improvement of stability seems to be at the cost of the oxygen permeability.<sup>14-16</sup> In addition to POM,<sup>17-21</sup> the perovskite membranes have been widely evaluated in the oxygen production,<sup>22,23</sup> the generation of oxygen enriched air,<sup>24</sup> the selective oxidation of hydrocarbons,<sup>25-27</sup> and for power plants with carbon sequestration.<sup>28,29</sup>

At the same time, different membrane geometries such as disks, tubes, monoliths, capillaries, and hollow fibers as full or graded materials have been developed. However, most of these geometries do not fulfill industrial requirements. For example, disk-shaped membranes that can be prepared quite easily by a pressing and sintering method show a low surface-to-volume ratio and significant problems associated with the high-temperature sealing.<sup>14</sup> As a result, tube membranes in the cm-scale were developed to reduce the engineering difficulties, especially the sealing problems. However, their small surface area to volume ratio makes them also unfavorable in practice. A very interesting concept to overcome these restrictions is the application of flat membranes stacked to larger units as proposed by Air Products and Chemicals.<sup>30</sup> Increasing activities can be observed in the preparation of oxygen ion conducting membranes in a hollow fiber geometry. Examples are the pioneering articles from the groups of Li and coworkers,<sup>31-36</sup> Liu et al.,<sup>37-39</sup> and Schiestel et al.,<sup>40-42</sup> as well as the articles by Truncel<sup>43</sup> and Luyten et al.<sup>44</sup> showing that thin-walled ceramic fibers can be prepared by wet-spinning. Such hollow fiber membranes possess several advantages: (1) a large membrane

area per unit volume for oxygen permeation (about  $2500\text{ m}^2$  per  $\text{m}^3$  permeator assuming a bunch of fibers of  $0.75\text{ mm}$  diameter); (2) high oxygen permeation flux due to thin walls; and (3) easy assembly for large-scale module fabrications. These advantages recommend the hollow fiber as potential and promising configuration in future industrial applications.

In previous studies, we investigated the possible reaction pathway of the POM in a hollow fiber membrane reactor<sup>45</sup> and the effect of carbon deposit on the stability of fiber during the POM reaction.<sup>46</sup> In this article, the performance of the  $BaCo_xFe_yZr_zO_{3-\delta}$  ( $x + y + z = 1$ , BCFZ) hollow fiber in the POM reaction with/without catalyst and coated/packed catalyst as well as the operation stability of the hollow fiber membrane reactor for different catalyst arrangements are investigated in detail. The aim of the present article is to optimize the operation conditions and the catalyst arrangements for the POM in the hollow fiber membrane reactor. The material BCFZ was chosen because it can be operated steadily for POM for more than 2200 h and was the best material reported in open literatures so far.<sup>47</sup>

## Experimental

The dense  $BaCo_xFe_yZr_zO_{3-\delta}$  (BCFZ,  $x + y + z = 1$ ) perovskite hollow fiber membrane was prepared by phase inversion spinning followed by sintering.<sup>40-42</sup> Two ends of the hollow fiber were coated by Au paste (C5754, Heraeus). After sintered at  $950^\circ\text{C}$  for 5 h, a dense Au film was obtained. Therefore, such Au-coated hollow fibers can be sealed outside the oven at room temperature and the uncoated part can be kept in the middle of the oven ensuring isothermal conditions for the oxygen transport. Air of  $150\text{ ml/min}$  was fed to the core side and a mixture of  $CH_4$  and He was fed to the shell side. Under these conditions, the fiber was subjected to synthesis gas production in different reactor configurations, as shown in Figure 1. In Configuration A, no catalyst was used. In Configuration B, a commercial Ni-based steam reforming (SR) catalyst (Süd-Chemie) was coated on the fiber by a dip-coating procedure. In Configuration C,  $0.4\text{ g}$  Ni-based SR catalyst was packed around the active oxygen transporting part of the hollow fiber membrane. In Configuration D,  $0.6\text{ g}$  Ni-based SR catalyst was packed around and behind the uncoated part of the hollow fiber membrane. In Configuration E,  $0.4\text{ g}$  Ni-based SR catalyst was packed only behind the active zone of the hollow fiber membrane. The gas composition at the outlet of the shell side was determined by gas chromatography (Agilent 6890 with a Carboxen 1000 column supplied by Supelco). The  $H_2O$  amount was determined from the hydrogen atom balance.  $CH_4$  conversion ( $X_{CH_4}$ ) and product selectivities ( $S_i$ ) were defined as follows:

$$X_{CH_4} = 100 - \frac{F_{CH_4}^{out}}{F_{CH_4}^{in}} \times 100\% \quad (1)$$

$$S_i = \frac{n_i F_i}{F_{CH_4}^{in} - F_{CH_4}^{out}} \times 100\% \quad (2)$$

where  $n_i$  is the number of carbon atoms in the carbon-containing product molecules  $i$  and  $F_i$  is the flow rate of species  $i$  in  $\text{ml/min}$ , respectively.

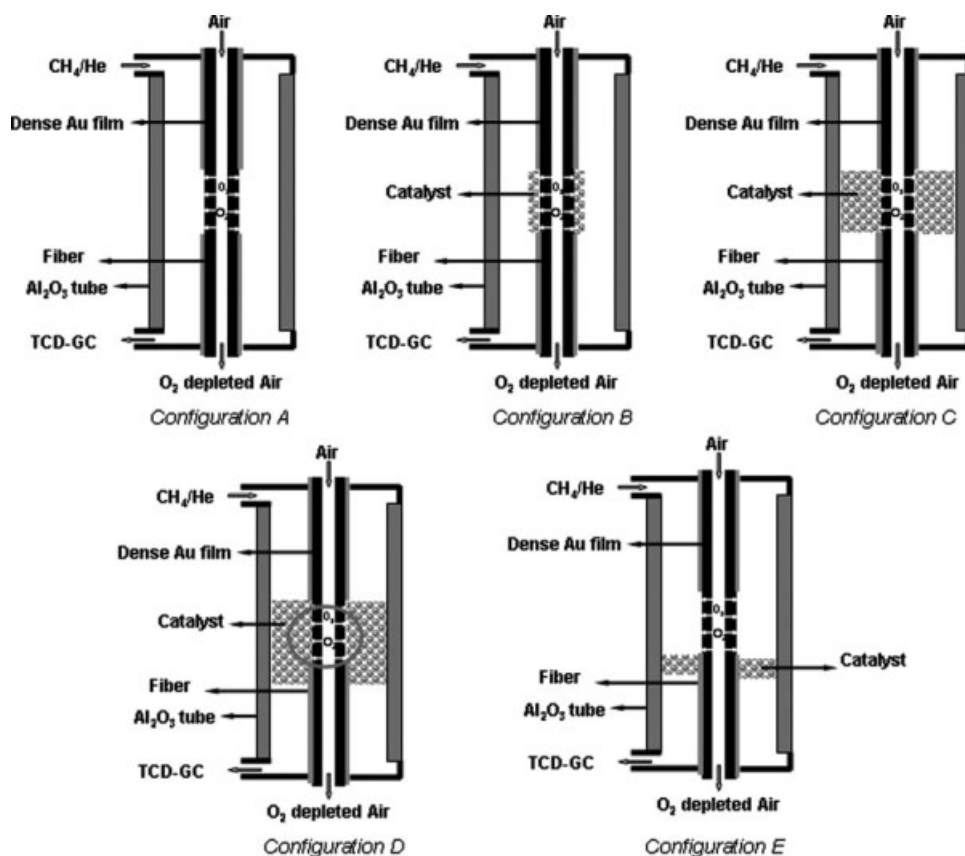


**Figure 1. Schematic diagram of different operation modes of BCFZ hollow fiber membrane reactor for POM.**  
The circle indicates the broken position of the BCFZ fiber during POM.

## Results and Discussion

### *POM performance in the BCFZ hollow fiber membrane reactor without catalyst (Configuration A)*

Perovskites show some catalytic activity and selectivity to light hydrocarbons, for example, for the POM, the oxidative coupling of methane and the oxidative dehydrogenation of ethane. Especially in the oxidative coupling of methane, perovskites show a rather high selectivity to  $C_2$ .<sup>48–50</sup> Therefore, it is informative to investigate the catalytic performance of the pure BCFZ hollow fiber itself without any additional catalyst.

Table 1 shows that under our reaction conditions only  $CO_2$  rather than other carbon-containing products ( $CO$  and  $C_{2+}$  hydrocarbons) were observed in the outflow when the BCFZ perovskite hollow fiber membrane was used in the POM at  $875^\circ C$  without any catalyst. The methane conversion is lower than 3%. Some amount of unreacted oxygen was found at the outlet of the membrane reactor together with unconverted methane.

Similar results were reported by Balachandran et al. who found that the permeated oxygen reacted with methane yielding  $CO_2$  and  $H_2O$  in a  $SrFeCo_{0.5}O_x$  tubular membrane reactor in the absence of a reforming catalyst.<sup>17</sup> The presence of  $CO_2$ ,  $H_2O$ ,  $CH_4$ , and  $O_2$  was also reported by Tsai et al. in the effluent gas of a  $La_{0.2}Ba_{0.8}Fe_{0.8}Co_{0.2}O_{3-\delta}$  disc-shaped membrane reactor without catalyst.<sup>51</sup> Therefore, it is

reasonable to use a suitable catalyst, which will catalyze the POM.

### *POM performance in the BCFZ hollow fiber membrane reactor coated with Ni-based SR catalyst (Configuration B)*

The surface of the hollow fiber was coated with the Ni-based SR-catalyst by dip-coating with a solution of the crashed catalyst. The modified hollow fiber membrane was characterized by field-emission scanning electron microscopy (Figure 2). From the cross-section it can be concluded that the catalyst layer is homogeneous and a few micrometer

**Table 1. Catalytic Performance of the BCFZ Hollow Fiber Membrane Reactor Without Reforming Catalyst in the POM**

Methane Concentration in the Feed (%)	CO Selectivity (%)	$CO_2$ Selectivity (%)	$CH_4$ Conversion (%)
10	0	100	1.5
20	0	100	2.6
50	1	99	2.4

Air flow rate on the shell side: 150 ml/min, total flow rate on the core side: 30 ml/min,  $CH_4$  concentration: 10–50 vol %, membrane surface area:  $3.3\text{ cm}^2$ , temperature:  $875^\circ C$ .

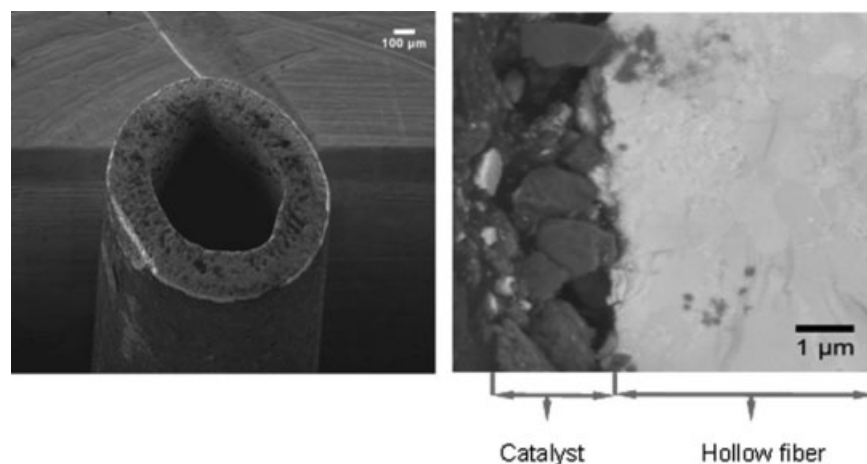


**Figure 2. SEM images of the modified hollow fiber membrane with Ni-based catalyst layer.**

thick. However, the catalyst layer shows some porosity, so oxygen permeation can occur.

Table 2 shows the CO and CO<sub>2</sub> selectivities as well as the methane conversion as a function of the methane flux on the shell side. Compared with Configuration A, almost no gaseous oxygen was found in the outflow of the reactor in Configuration B. The CH<sub>4</sub> conversion is much higher than that in the absence of the catalyst, which indicates that the permeated oxygen had reacted with methane thus decreasing the oxygen partial pressure and increasing the driving force for oxygen permeation. As a result, a higher oxygen flux through the hollow fiber membrane compared with the uncoated fiber is obtained. However, the CO selectivity is very low. This means that the deep oxidation of methane is the controlling reaction.

Dissanayake et al.<sup>52</sup> studied a Ni-based catalyst for the POM in the conventional packed bed reactor. They found that an effective catalyst bed consists of three different regions. In the first one at the reactor inlet, the catalyst is in contact with the CH<sub>4</sub>/O<sub>2</sub>/He feed mixture and the catalyst is present as NiAl<sub>2</sub>O<sub>4</sub>, which has only moderate activity for the complete oxidation of methane to CO<sub>2</sub> and H<sub>2</sub>O. In the second region NiO/Al<sub>2</sub>O<sub>3</sub> is present, where the complete oxidation of methane to CO<sub>2</sub> occurs, resulting in a strong temperature increase in this section of the bed. As a result of the complete consumption of O<sub>2</sub> in the second region, the catalyst in the third region consists of a reduced Ni/Al<sub>2</sub>O<sub>3</sub> phase. Formation of CO and H<sub>2</sub>, corresponding to the thermodynamic equilibrium at the catalyst bed temperature, occurs in this final region via reforming reactions of CH<sub>4</sub> with the CO<sub>2</sub> and H<sub>2</sub>O produced during the complete oxidation on the NiO/Al<sub>2</sub>O<sub>3</sub> phase.

In our experiment, a thin layer of Ni-based SR catalyst was coated on the surface of the hollow fiber membrane (see Figure 2). Because of the continuous oxygen permeation through the membrane, Ni can easily be oxidized to NiO. Therefore, the Ni species of the catalyst layer are presumably NiO or NiAl<sub>2</sub>O<sub>4</sub>, which are active for the total oxidation of methane to produce CO<sub>2</sub> and H<sub>2</sub>O instead of the POM to synthesis gas. So it can be easily understood that a lot of CO<sub>2</sub> was observed in the coated hollow fiber mem-

brane reactor. To increase the CO selectivity, more catalyst is needed for CH<sub>4</sub> reforming with CO<sub>2</sub> and H<sub>2</sub>O and additional catalyst will be packed in the section behind the active part of the hollow fiber membrane.

It should be pointed out that in Configuration B the coated BCFZ hollow fiber membrane survived only 5 h when it was operated as a reactor for the POM reaction at 875°C. One possible reason for this behavior is the high CO<sub>2</sub>-concentration near the membrane surface. Details of the effects of CO<sub>2</sub> on microstructure and oxygen permeation of a different perovskite are reported elsewhere.<sup>53</sup> The consideration of Ellingham diagrams allows estimating critical conditions for the operation of materials containing alkaline-earth cations.<sup>15,54</sup> For the conditions chosen in the experiments under discussion, it is reasonable to assume that the structure of the hollow fiber membrane was destroyed by BaCO<sub>3</sub> formation because of the high CO<sub>2</sub> partial pressure. An alternative explanation for the degradation of the fiber could be the local temperature increase near the membrane surface caused by the total oxidation of methane.

***POM performance in the BCFZ hollow fiber membrane reactor packed with Ni-based catalyst (Configurations C and D)***

The Ni-based SR catalyst was applied as a packed bed (~0.16 to 0.4 μm particle size) around the perovskite fiber

**Table 2. Catalytic Performance of the POM in the Modified BCFZ Hollow Fiber Membrane Reactor Coated with Ni-Based Catalyst According to Configuration B**

CH <sub>4</sub> Flow Rate (ml/min cm <sup>2</sup> )	CO Selectivity (%)	CO <sub>2</sub> Selectivity (%)	CH <sub>4</sub> Conversion (%)
5	0.1	99.9	76.5
10	0.1	99.9	59.2
15	0.2	99.8	63.7
20	7.2	92.8	63.2
25	9.7	90.3	56.7

Air flow rate on the core side: 150 ml/min, total flow rate on the shell side: 10–50 ml/min, methane concentration: 50%, membrane surface area: 3.3 cm<sup>2</sup>, catalyst amount: 0.4 g, temperature: 875°C.



**Table 3. Catalytic Performance of the Membrane Reactor with a BCFZ Hollow Fiber with a Ni-Based SR Catalyst (Configurations C and D) in the POM Reaction**

Catalyst Position	Temperature (°C)	CO Selectivity (%)	CO <sub>2</sub> Selectivity (%)	CH <sub>4</sub> Conversion (%)	H <sub>2</sub> /CO Ratio
Around the fiber	825	81.6	18.4	38.7	1.86
	850	79.4	20.6	49	1.85
	875	74.6	25.4	60.9	1.85
	900	60.6	39.4	65.9	1.64
	925	49.1	50.9	71.4	1.4
Around and behind the fiber	825	98	2	43.9	2.33
	850	98.4	1.6	59.6	2.38
	875	97.8	2.2	85	2.48
	900	97.1	2.9	92.2	2.22
	925	96.6	3.4	95.8	2.08

Air flow rate on the shell side: 150 ml/min, total flow rate on the shell side: 20 ml/min, methane concentration 50 %, catalyst amount: 0.4 g (for cf. C) and 0.6 g (cf. D), membrane surface area: 0.56 cm<sup>2</sup>.

(shell side, Configuration C). From Table 3 it can be seen that the CH<sub>4</sub> conversion is considerably higher than in the absence of catalyst (Table 1). This result suggests that the oxygen permeation flux in Configuration C is much higher than without Ni-catalyst. Furthermore, the CO selectivity is much higher than in Configuration B. However, the CO selectivity is lower than 82% and decreases with increasing temperature. A considerable amount of unreacted methane is also found. At 925°C, both CO<sub>2</sub> and CO selectivities reach 50% at only 70% CH<sub>4</sub> conversion. These experimental findings indicate that the methane reforming with the produced CO<sub>2</sub> and H<sub>2</sub>O was not complete.

In the case of additional catalyst behind the active part of the membrane (Configuration D in Figure 1), a considerable improvement can be stated and CO and H<sub>2</sub> become the main reaction products (cf. Table 3). At 925°C, the CO selectivity is above 97% at roughly 96% CH<sub>4</sub> conversion and the H<sub>2</sub>/CO ratio is around 2.08 as expected for POM. The temperature increase in the CH<sub>4</sub> conversion is ascribed to the temperature-accelerated oxygen permeation flux.

The changes in the catalytic performance of the membrane reactor in the presence of the Ni-based SR catalyst can be explained as follows: As the BCFZ membrane has very low intrinsic activity for methane oxidation (Table 1), methane conversion occurs nearly exclusively over the Ni-based SR catalyst. Previous research showed that synthesis gas formation from methane in a mixed conducting perovskite membrane reactor may be called an “oxidation-reforming process,” that is, a total oxidation followed by steam and dry reforming steps. In the second step, the concentration of H<sub>2</sub>O and CO<sub>2</sub> is reduced by further SR and dry reforming of unreacted CH<sub>4</sub> giving CO and H<sub>2</sub>.<sup>21</sup> By applying more and more catalyst, the catalyst-based residence time is enlarged so this oxidation-reforming-process can be completed.

#### **Operational stability and performance of the membrane reactor in the POM (Configurations D and E)**

The stability of the hollow fiber membrane was studied for two Configurations (D and E in Figure 1). Figure 3 shows the stability measurements for the POM reaction in the hollow fiber membrane reactor at 875°C in the Configuration D. CO and H<sub>2</sub> are the main reaction products. CO selectivity of 97% with CH<sub>4</sub> conversion of 96% is obtained

and the H<sub>2</sub>/CO ratio is 2.0 as expected for the POM. However, the hollow fiber membrane was broken after 9 h time on stream. The defect occurred at a position in which the membrane was in contact with the Ni-based SR catalyst (as shown in Configuration D in Figure 1 with a circle).

The destroyed membrane was studied by scanning electron microscopy (SEM) and energy-dispersive X-ray spectroscopy (EDXS). As can be seen from Figure 4, the fiber became amorphous and porous, especially on its outer parts in contact with the catalyst/methane side. From the initial wall thickness of 170 μm, only 40 μm remained as a dense perovskite phase showing some cracks. About 110 μm of the fiber in contact with the catalyst and about 20 μm on the air side became porous. Different positions of the spent hollow fiber membrane were examined by EDXS. Surprisingly, in the outer and to some extent in the middle parts of the cross section of the porous fiber, Al from the SR catalyst was found. The Al diffusion into the perovskite fiber may be a possible reason for its failure. No Al was observed in the spectrum of the inner intact part (40 μm) of the hollow fiber membrane.

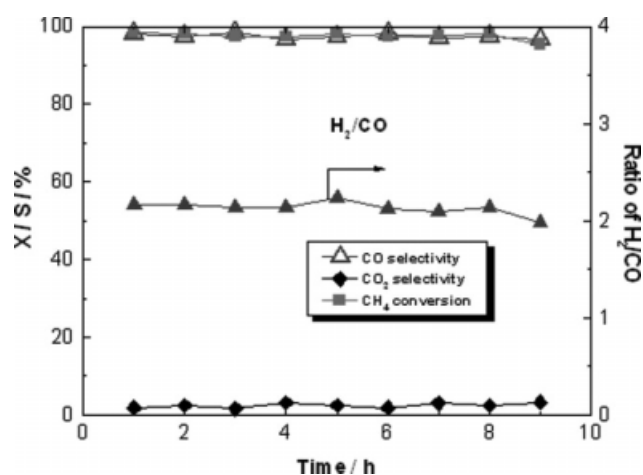


**Figure 3. Performance and stability of the fiber during POM reaction in the Configuration D.**

Air flow rate on the core side: 150 ml/min, total flow rate on the shell side: 20 ml/min, methane concentration: 50%, catalyst amount: 0.6 g, membrane surface area: 0.56 cm<sup>2</sup>, temperature: 875°C.

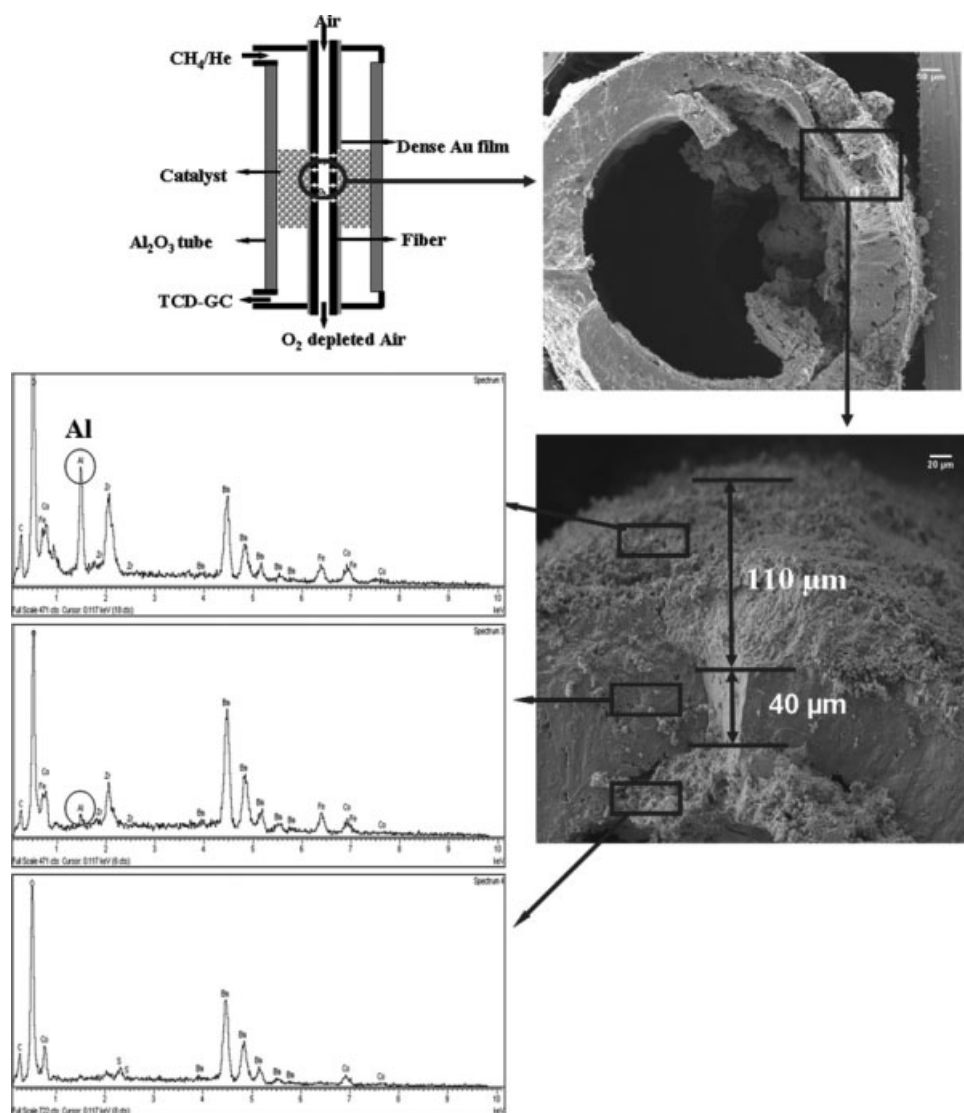


Figure 4. SEM and EDXS of spent fiber after 9 h operation in the POM in Configuration D (cf. Figure 3).

By avoiding physical contact between fiber and catalyst, the stability of the membrane in the POM reaction should be improved. In Configuration E, the catalyst was positioned only behind the oxygen permeation zone where the fiber was coated with Au. Figure 5 shows the stability measurements for the POM reaction in the hollow fiber membrane reactor at 875°C. A CO selectivity of above 90% with a methane conversion of 93% and a H<sub>2</sub>/CO ratio around 2 are obtained. It is obvious that the fiber in this case survives longer than in Configuration D because the Au film avoids the contact of catalyst and fiber. Compared with the other configurations, the stability of the fiber in Configuration E is significantly improved. By separating catalyst and fiber, the hollow fiber membrane reactor could be steadily operated more than 300 h in the POM.<sup>55</sup>

It follows from literature analysis that in most of the POM studies the catalyst was in direct contact with the membrane and usually problems such as the impact of reducing atmospheres and solid-state reactions between catalyst and membrane were not mentioned. In this study, we found as the

best choice to pack the catalyst behind the membrane. At first sight, a coupling of the three steps (i) oxygen permeation, (ii) membrane total oxidation, and (iii) carbon dioxide/SR with methane look promising for several reasons. The continuous consumption of the permeated oxygen will establish a constant high driving force for the oxygen flux and the combination of the exothermal combustion with the endothermal reforming could guarantee optimal heat management in Configurations C and D. However, there are also reasons speaking against these concepts, as high concentrations of reducing gases produced by the reforming step (CO, H<sub>2</sub>) could reduce the BCFZ fiber and the direct contact between catalyst and fiber can initiate an exchange of mobile species between BCFZ and catalyst by solid-state ion diffusion (Fe, Co).

Obviously, in our best Configuration E, the oxygen permeation zone of the BCFZ hollow fiber is in contact with methane and one could assume a reduction of the perovskite by methane. However, this reduction does not take place, most probably due to a continuous flow of oxygen released from

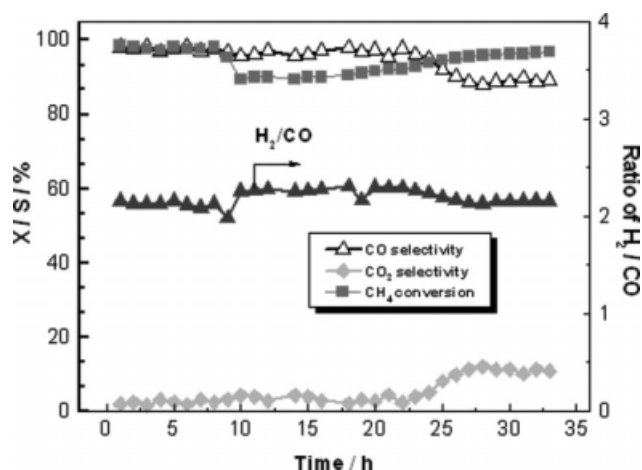


**Figure 5. Stability of the fiber during POM reaction in the Configuration E.**

Air flow rate on the core side: 150 ml/min, total flow rate on the shell side: 20 ml/min, methane concentration: 50%, catalyst amount: 0.4 g, membrane surface area: 0.56 cm<sup>2</sup>, temperature: 875°C.

the perovskite. With other words, there is always a nonzero oxygen partial pressure at the perovskite surface which means that no pure methane as reducing agent is in contact with the perovskite. Furthermore, the benefit of Configuration E is that no major CO<sub>2</sub>, CO, or H<sub>2</sub> concentrations are in contact with the unprotected perovskite fiber because the formation of these products is kinetically suppressed in the homogeneous gas phase reaction without catalyst. And even if these products are formed, the oxygen flow from the perovskite surface would reduce their impact.

In the conventional technology, pure oxygen is needed for the POM. This oxygen is conventionally produced by cryogenic fractionation technology, which requires a large-scale plant and high-operation costs. In the membrane reactor technology, the membrane can be used to in-situ produce pure oxygen from air which is competitive to the conventional technology.

## Conclusion

The POM to syngas was investigated at 825–925°C using a membrane reactor based on BCFZ hollow fibers with and without SR catalyst in different catalyst arrangements. It was found that to get a high CO selectivity, an additional amount of catalyst was needed behind the active membrane area to ensure that the reforming reactions can take place completely. Stability studies of the hollow fiber membrane in the POM reaction showed that the stability of the fiber can be significantly improved if the contact between fiber and catalyst is avoided. A stable reactor concept is proposed with an arrangement of the reforming catalyst behind the oxygen permeation zone. In this case, the BCFZ perovskite is not attacked by strongly reducing components like CO and H<sub>2</sub> or by carbonate formation with CO<sub>2</sub> because the formation of these components at the perovskite site is kinetically suppressed without catalyst. Furthermore, the continuous release of oxygen from the perovskite surface results in a nonzero

oxygen partial pressure at the surface and prevents a reduction of the perovskite by, for example, methane.

## Acknowledgments

The authors gratefully acknowledge the financial support of the German BMBF for project 03C0343A under the auspices of ConNeCat. The authors acknowledge gratefully financial support from the National Natural Science Foundation of China (nos. 20706020, U0834004) and from the Deutsche Forschungsgemeinschaft (DFG) under grant FE 928/1-1.

## Literature Cited

- Agee M. Petroleum. *Economist*. January 20–21, 2002.
- Weber WJ, Stevenson JW, Armstrong TR, Pederson LR. Processing and electrochemical properties of mixed conducting La<sub>1-x</sub>A<sub>x</sub>Co<sub>1-y</sub>Fe<sub>y</sub>O<sub>3-δ</sub> (A = Sr, Ca). *Mat Res Soc Proc.* 1995;369:395–400.
- Dong H, Xiong GX, Shao ZP, Cong Y, Yang WS. Partial Oxidation of methane to syngas in a mixed-conducting oxygen permeable membrane reactor. *Chin Sci Bull.* 2000;45:224–226.
- Udovich CA. Ceramic membrane reactors for the conversion of natural gas to syngas. *Stud Surf Sci Catal.* 1998;119:417–422.
- Teraoka Y, Zhang HM, Furukawa S, Yamazoe N. Oxygen permeation through perovskite-type oxides. *Chem Lett.* 1985;11:1743–1746.
- Shao ZP, Yang WS, Cong Y, Dong H, Tong JH, Xiong GX. Investigation of the permeation behaviour and stability of a Ba<sub>0.5</sub>Sr<sub>0.5</sub>Co<sub>0.8</sub>Fe<sub>0.2</sub>O<sub>3-δ</sub> oxygen membrane. *J Membr Sci.* 2000;172:177–188.
- Shao ZP, Dong H, Xiong GX, Gong Y, Yang WS. Performance of a mixed-conducting ceramic membrane reactor with high oxygen permeability for methane conversion. *J Membr Sci.* 2001;183:181–192.
- Shao ZP, Xiong GX, Cong Y, Yang WS. Synthesis and oxygen permeation study of novel perovskite-type BaBi<sub>1-x</sub>Co<sub>0.2</sub>Fe<sub>0.8-x</sub>O<sub>3-δ</sub> ceramic membranes. *J Membr Sci.* 2000;164:167–176.
- Ishihara T, Yamada T, Arikawa H, Nishiguchi H, Takita Y. Mixed electronic-oxide ionic conductivity and oxygen permeating property of Fe-, Co- or Ni-doped LaGaO<sub>3</sub> perovskite oxide. *Solid State Ionics.* 2000;135:631–636.
- Ishihara T, Yamada T, Arikawa H, Nishiguchi H, Takita Y. Fe doped LaGaO<sub>3</sub> perovskite oxide as an oxygen separating membrane for CH<sub>4</sub> partial oxidation. *Solid State Ionics.* 2002;152:709–714.
- Kharton VV, Naumovich EN, Kovalevsky AV, Viskup AP, Figueiredo FM, Bashmakov IA, Marques FMB. Mixed electronic and ionic conductivity of LaCo(M)O<sub>3</sub> (M = Ga, Cr, Fe or Ni) IV. Effect of preparation method on oxygen transport in LaCoO<sub>3-δ</sub>. *Solid State Ionics.* 2000;138:135–148.
- Shaula AL, Kharton VV, Marques FMB. Ionic and electronic conductivities, stability and thermal expansion of La<sub>10-x</sub>(Si, Al)<sub>6</sub>O<sub>26±δ</sub> solid electrolytes. *Solid State Ionics.* 2006;177:1725–1728.
- Wang HH, Tablet C, Feldhoff A, Caro J. A cobalt-free oxygen-permeable membrane based on the perovskite-type oxide Ba<sub>0.5</sub>Sr<sub>0.5</sub>Zn<sub>0.2</sub>Fe<sub>0.8</sub>O<sub>3-δ</sub>. *Adv Mater.* 2005;17:1785–1788.
- Zhu XF, Wang HH, Yang WS. Novel cobalt-free oxygen permeable membrane. *Chem Commun.* 2004;9:1130–1131.
- Feldhoff A, Martynczuk J, Wang HH. Advanced Ba<sub>0.5</sub>Sr<sub>0.5</sub>Zn<sub>0.2</sub>Fe<sub>0.8</sub>O<sub>3-δ</sub> perovskite-type ceramics as oxygen selective membranes: evaluation of the synthetic process. *Prog Solid State Chem.* 2007;35:339–353.
- Chen ZH, Shao ZP, Ran R, Zhou W, Zeng PY, Liu SM. A dense oxygen separation membrane with a layered morphologic structure. *J Membr Sci.* 2007;300:182–190.
- Balachandran U, Dusek JT, Maiya PS, Ma B, Mieville RL, Kleefisch MS, Udovich CA. Ceramic membrane reactor for converting methane to syngas. *Catal Today.* 1997;36:265–272.
- Gu XH, Jin WQ, Chen CL, Xu NP, Shi J, Ma YH. YSZ-SrCo<sub>0.4</sub>Fe<sub>0.6</sub>O<sub>3-δ</sub> membranes for the partial oxidation of methane to syngas. *AIChE J.* 2002;48:2051–2060.
- Chen CS, Feng SJ, Ran S, Zhu DC, Liu W, Bouwmeester HJM. Conversion of methane to syngas by a membrane-based oxidation-reforming process. *Angew Chem Int Ed Engl.* 2003;42:5196–5198.
- Bouwmeester HJM. Dense ceramic membranes for methane conversion. *Catal Today.* 2003;82:141–150.

21. Gu XH, Yang L, Tan L, Jin WQ, Zhang LX, Xu NP. Modified operating mode for improving the lifetime of mixed-conducting ceramic membrane reactors in the POM environment. *Ind Eng Chem Res.* 2003;42:795–801.
22. Vente JF, Haije WG, Rak ZS. Performance of functional perovskite membranes for oxygen production. *J Membr Sci.* 2006;276:178–184.
23. Wu ZT, Jin WQ, Xu NP. Oxygen permeability and stability of  $\text{Al}_2\text{O}_3$ -doped  $\text{SrCo}_{0.8}\text{Fe}_{0.2}\text{O}_{3-\delta}$  mixed conducting oxides. *J Membr Sci.* 2006;279:320–327.
24. Wang HH, Werth S, Schiestel T, Caro J. Perovskite hollow-fiber membranes for the production of oxygen-enriched air. *Angew Chem Int Ed Engl.* 2005;44:6906–6909.
25. Wang HH, Cong Y, Yang WS. High selectivity of oxidative dehydrogenation of ethane to ethylene in an oxygen permeable membrane reactor. *Chem Commun.* 2002;14:1468–1469.
26. Rebeilleau-Dassonneville M, Rosini S, van Veen AC, Farrusseng D, Mirodatos C. Oxidative activation of ethane on catalytic modified dense ionic oxygen conducting membranes. *Catal Today.* 2005;104:131–137.
27. Akin FT, Lin YS. Selective oxidation of ethane to ethylene in a dense tubular membrane reactor. *J Membr Sci.* 2002;209:457–467.
28. Ren JY, Fan YQ, Egolfopoulos FN, Tsotsis TT. Membrane-based reactive separations for power generation applications: oxygen lancing. *Chem Eng Sci.* 2003;58:1043–1052.
29. Fan YQ, Ren JY, Onstot W, Pasale J, Tsotsis TT, Egolfopoulos FN. Reactor and technical feasibility aspects of a  $\text{CO}_2$  decomposition-based power generation cycle, utilizing a high-temperature membrane reactor. *Ind Eng Chem Res.* 2003;42:2618–2626.
30. Holmes MJ, Orhn TR, Chen CMP. Ion transport membrane module and vessel system with directed internal gas flow. Eur. Patent EP1676811, 2006.
31. Tan XY, Liu Y, Li K. Mixed conducting ceramic hollow-fiber membranes for air separation. *AIChE J.* 2005;51:1991–2000.
32. Tan XY, Liu Y, Li K. Preparation of LSCF ceramic hollow-fiber membranes for oxygen production by a phase-inversion/sintering technique. *Ind Eng Chem Res.* 2005;44:61–66.
33. Tan XY, Li K. Oxygen production using dense ceramic hollow fiber membrane modules with different operating modes. *AIChE J.* 2007;53:838–845.
34. Tan XY, Liu SM, Li K. Preparation and characterization of inorganic hollow fiber membranes. *J Membr Sci.* 2001;188:87–95.
35. Liu SM, Tan XY, Li K, Hughes R. Preparation and characterisation of  $\text{SrCe}_{0.95}\text{Yb}_{0.05}\text{O}_{2.975}$  hollow fiber membranes. *J Membr Sci.* 2001;193:249–260.
36. Liu SM, Li K, Hughes R. Preparation of  $\text{SrCe}_{0.95}\text{Yb}_{0.05}\text{O}_{3-\delta}$  perovskite for use as a membrane material in hollow fiber fabrication. *Mater Res Bull.* 2004;39:119–133.
37. Liu SM, Gavallas GR. Oxygen selective ceramic hollow fiber membranes. *J Membr Sci.* 2005;246:103–108.
38. Liu SM, Gavallas GR. Preparation of oxygen ion conducting ceramic hollow-fiber membranes. *Ind Eng Chem Res.* 2005;44:7633–7637.
39. Liu SM, Tan XY, Shao ZP, da Costa JCD.  $\text{Ba}_{0.5}\text{Sr}_{0.5}\text{Co}_{0.8}\text{Fe}_{0.2}\text{O}_{3-\delta}$  ceramic hollow-fiber membranes for oxygen permeation. *AIChE J.* 2006;52:3452–3461.
40. Schiestel T, Kilgus M, Peter S, Caspary KJ, Wang HH, Caro J. Hollow fibre perovskite membranes for oxygen separation. *J Membr Sci.* 2005;258:1–4.
41. Kilgus M, Wang HH, Werth S, Caro J, Schiestel T. Dense perovskite hollow fibre membranes. *Desalination.* 2006;199:355–356.
42. Tablet C, Grubert G, Wang HH, Schiestel T, Schroeder M, Langanke B, Caro J. Oxygen permeation study of perovskite hollow fiber membranes. *Catal Today.* 2005;104:126–130.
43. Truncel M. Fabrication of zirconia- and ceria-based thin-wall tubes by thermoplastic extrusion. *J Eur Ceram Soc.* 2004;24:645–651.
44. Luyten J, Buekenhoudt A, Adriansens W, Coymans J, Weyten H, Servaes F, Leysen R. Preparation of  $\text{LaSrCoFeO}_{3-x}$  membranes. *Solid State Ionics.* 2000;135:637–642.
45. Wang HH, Tablet C, Schiestel T, Werth S, Caro J. Partial oxidation of methane to syngas in a perovskite hollow fiber membrane reactor. *Catal Commun.* 2006;7:907–912.
46. Kleinert A, Feldhoff A, Schiestel T, Caro J. Novel hollow fibre membrane reactor for the partial oxidation of methane. *Catal Today.* 2006;118:44–51.
47. Tong JH, Yang WS, Cai R, Zhu BC, Lin LW. Novel and ideal zirconium-based dense membrane reactors for partial oxidation of methane to syngas. *Catal Lett.* 2002;78:129–137.
48. Akin FT, Lin YS. Oxidative coupling of methane in dense ceramic membrane reactor with high yields. *AIChE J.* 2002;48:2298–2306.
49. Xu SJ, Thomson WJ. Perovskite-type oxide membrane for the oxidative coupling of methane. *AIChE J.* 1997;43:2731–2740.
50. Elshof JE, Bouwmeester HJM, Verweij H. Oxidative coupling of methane in a mixed-conducting perovskite membrane reactor. *Appl Catal Gen: A.* 1995;130:195–212.
51. Tsai CY, Dixon AG, Moser WR, Ma Y. Dense perovskite membrane reactors for partial oxidation of methane to syngas. *AIChE J.* 1997;43:2741–2750.
52. Dissanayake D, Rosynek MP, Kharas KCC, Lunsford JH. Partial oxidation of methane to carbon monoxide and hydrogen over a  $\text{Ni}/\text{Al}_2\text{O}_3$  catalyst. *J Catal.* 1991;132:117–127.
53. Arnold M, Wang, HH, Martynczuk J, Feldhoff A. In-situ study of the reaction sequence in the sol-gel synthesis of a  $(\text{Ba}_{0.5}\text{Sr}_{0.5})(\text{Co}_{0.8}\text{Fe}_{0.2})\text{O}_{3-\delta}$  perovskite by X-ray diffraction and transmission electron microscopy. *J Am Ceram Soc.* 2007;90:3651–3655.
54. Feldhoff A, Martynczuk J, Arnold, M, Wang HH. The sol-gel synthesis of perovskites by an EDTA/citrate complexing method involves nanoscale solid state reactions. *Solid State Sci.* 2008;10:689–701.
55. Caro J, Caspary KJ, Hamel C, Hoting B, Kölsch P, Langanke B, Nassauer K, Noack M, Schiestel T, Schroeder M, Byun YC, Seidel-Morgenstern A, Tsotsas E, Voigt I, Wang HH, Warsitz R, Werth S, Aurel W. Catalytic membrane reactors for partial oxidation using perovskite hollow fiber membranes and for partial hydrogenation using a catalytic membrane reactor. *Ind Eng Chem Res.* 2007;46:2286–2294.

Manuscript received Apr. 24, 2008, and revision received Jan. 7, 2009.